Physics – Uspekhi **57** (9) 897 – 902 (2014)

METHODOLOGICAL NOTES PACS numbers: 61.50.Ks, 61.66.Bi, 62.20.D –, **62.50. – p**

Elastic phase transitions in metals at high pressures

Yu Kh Vekilov, O M Krasilnikov, M P Belov, A V Lugovskoy

DOI: 10.3367/UFNe.0184.201409d.0967

Contents

Abstract. Crystalline lattices can become unstable to uniform shear strains, which may lead to a structural transformation to less symmetric structures. Transitions of this type are called elastic phase transitions. In this paper, elastic phase transitions in metals with cubic and hexagonal structures are considered. The relation between the elastic constants of second, third, and fourth order corresponding to the case of a first-order elastic phase transition are given. As an example, the structural transformation in vanadium, which is experimentally observed at $P \approx 69$ GPa, and the possibility of structural transformation in molybdenum at P higher than 700 GPa are analyzed.

1. Introduction

Structural phase transitions under high pressures (comparable in magnitude to the bulk modulus) are becoming the subject of intense research [1–3], because diamond anvil cell pressures of 500–600 GPa [4] are already available and because, with the structure identification methods using synchrotron X-ray diffraction, the real-time structure monitoring of high-pressure phases has become possible. Such structural changes are special because, in contrast to low pressure, where transitions occur to a close-packed high-symmetry structure [5], high-pressure phases in ultra-high pressure experiments are often less symmetric and less densely packed [1, 2]. A possible explanation is that increasing the pressure makes the crystal lattice unstable to small uniform deformations. It was shown in [6] using the density functional method that under high compression, the shear elastic constants of Na and K exhibit a strong softening behavior, resulting in the transition to a spontaneous deformation state of lower symmetry than the initial phase.

Yu Kh Vekilov, O M Krasilnikov, M P Belov, A V Lugovskoy National Research Technological University 'MISiS',
Leninskii prosp. 4, 119049 Moscow, Russian Federation
E-mail: omkras@mail.ru; andrey.lugovskoy@gmail.com

Received 3 December 2013, revised 19 December 2013
Uspekhi Fizicheskikh Nauk **184** (9) 967 – 973 (2014)
DOI: 10.3367/UFNr.0184.201409d.0967
Translated by E G Strel'chenko; edited by A M Semikhatov

Although elastic deformations are almost a universal feature of solid-state phase transitions, deformation is in most cases not an order parameter but rather a quantity related to the order parameter via striction interaction. In the structural transformations to be discussed here, deformation does represent an order parameter. To emphasize this point, the term 'elastic phase transitions' was introduced by Khmel'nitskii [7] (see also [8]). In these transitions, the number of atoms in a unit cell remains unchanged, the point symmetry group of the new phase is a subgroup of the point group of the initial phase, and translational symmetry is preserved [9]. It is shown in [7, 10] that critical phenomena in elastic phase transitions are strongly suppressed, and Landau's phase transition theory [11] is therefore applicable with finite deformation tensor components as order parameters. A considerable body of literature is available [8, 12] on temperature change (at atmospheric pressure) as another possible cause of elastic phase transitions (martensitic transformations). Here, we discuss the details of pressure-induced elastic phase transitions.

2. Crystal lattice stability and deformation phase transitions

Landau's theory of phase transitions assumes that a thermodynamic potential near the transition point can be expanded in a power series in order parameter components. For a system at a temperature T and pressure P, the relevant thermodynamic potential is the Gibbs free energy G. Structural transformations involve small, but finite lattice deformations, and therefore, to include the entire range of nonlinear effects, a convenient choice for the order parameter is the components of the Lagrange finite deformation tensor η_{ij} [13]. We expand G in terms of η_{ij} near the equilibrium state at given P and T. We assume the spontaneous deformations η_{ij} to be isothermal. Then the change $\Delta G = G(P, T, \eta) - G(P, T, 0)$ per unit volume in the initial state (V_0) has the form

$$\frac{\Delta G}{V_0} = \frac{1}{2}\,\tilde{C}_{ijkl}\,\eta_{ij}\,\eta_{kl} + \frac{1}{6}\,\tilde{C}_{ijklmn}\,\eta_{ij}\,\eta_{kl}\,\eta_{mn} + \frac{1}{24}\,\tilde{C}_{ijklmnpq}\,\eta_{ij}\,\eta_{kl}\,\eta_{mn}\,\eta_{pq} + \ldots . \quad (1)$$

Table 1. Strain-induced phase transitions under pressure in crystals of a cubic (1–3) and hexagonal (4–6) structure.

No.	Spontaneous strain	q	v	w	Symmetry change at transition
1	$-\eta_{11} = -\eta_{22} = 0{,}5\eta_{33} = \eta$	$6(\tilde{C}_{11} - \tilde{C}_{12})$	$3(\tilde{C}_{111} - 3\tilde{C}_{112} + 2\tilde{C}_{123})$	$3(\tilde{C}_{1111} - 4\tilde{C}_{1112} + 3\tilde{C}_{1122})$	$\Gamma_c \to \Gamma_q$ $\Gamma_c^f, \Gamma_c^v \to \Gamma_q^v$
2	$\eta_{11} = -\eta_{22} = \eta$	$2(\tilde{C}_{11} - \tilde{C}_{12})$	0 *	$(\tilde{C}_{1111} - 4\tilde{C}_{1112} + 3\tilde{C}_{1122})/3$	$\Gamma_c \to \Gamma_0$ $\Gamma_c^f, \Gamma_c^v \to \Gamma_o^v$
3	$\eta_{12} = \eta_{13} = \eta_{23} = \eta/2$	$3\tilde{C}_{44}$	$3\tilde{C}_{456}$	$(\tilde{C}_{4444} + 6\tilde{C}_{4455})/2$	$\Gamma_c, \Gamma_c^f, \Gamma_c^v \to \Gamma_{rh}$
4	$\eta_{11} = -\eta_{22} = \eta$	$\tilde{C}_{11} - \tilde{C}_{12}$	$2(\tilde{C}_{111} - \tilde{C}_{222})/3$	$2\tilde{C}_{6666}/3$	$\Gamma_h \to \Gamma_o^b$
5	$\eta_{23}(\eta_{13}) = \eta$	$\tilde{C}_{44}$	0	$2\tilde{C}_{4444}/3$	$\Gamma_h \to \Gamma_m$
6	$\eta_{12} = \eta$	$\tilde{C}_{11} - \tilde{C}_{12}$	0	$2\tilde{C}_{6666}/3$	$\Gamma_h \to \Gamma_o^b$
* Due to deformation symmetry.					

Here and hereafter, summation over repeated indices from 1 to 3 is implied. The linear term is absent because the system is in equilibrium. Here, the quantities

$$\tilde{C}_{ijkl\ldots} = \frac{1}{V_0}\left(\frac{\partial^n G}{\partial\eta_{ij}\partial\eta_{kl}\ldots}\right)_0 \tag{2}$$

are the nth-order $(n = 2, 3, 4)$ isothermal effective elastic constants of a loaded crystal under a fixed loading at a temperature T [14]. In the absence of loading, $\tilde{C}_{ijkl\ldots}$ are identical to the usual elastic constants. When using $\tilde{C}_{ijkl\ldots}$, all the equations of elastic theory remain the same, independent of whether the crystal is under loading. In particular, the stability equations for a uniformly deformed loaded crystal are identical to the well-known Born conditions.

At given P and T, the system is in equilibrium if the quadratic form in Eqn (1) is positive definite. As a result, for the three most common metallic structures — body-centered cubic (bcc), face-centered cubic (fcc) and hexagonal close-packed (hcp) — the following stability conditions are obtained for uniform hydrostatic compression and shear. For a cubic crystal, we have

$$\tilde{C}_{11} + 2\tilde{C}_{12} > 0\,, \tag{3a}$$

$$\tilde{C}_{11} - \tilde{C}_{12} > 0\,, \tag{3b}$$

$$\tilde{C}_{44} > 0\,. \tag{3c}$$

Similarly, for a hexagonal crystal,

$$\tilde{C}_{33}(\tilde{C}_{11} + \tilde{C}_{12}) - 2\tilde{C}_{13}^2 > 0\,, \tag{4a}$$

$$\tilde{C}_{11} - \tilde{C}_{12} > 0\,, \tag{4b}$$

$$\tilde{C}_{44} > 0\,, \tag{4c}$$

$$\tilde{C}_{66} = \frac{\tilde{C}_{11} - \tilde{C}_{12}}{2} > 0\,. \tag{4d}$$

Here, $\tilde{C}_{\alpha\beta}$ are the effective second-order elastic constants in the Voigt notation; α and β can take values from 1 to 6 in accordance with the rule $11 \to 1$, $22 \to 2$, $33 \to 3$, $23 \to 4$, $13 \to 5$, $12 \to 6$. We note that conditions (4) also hold for the tetragonal lattice, except that Eqn (4d) becomes $\tilde{C}_{66} > 0$ because in that case, $\tilde{C}_{66} \neq (\tilde{C}_{11} - \tilde{C}_{12})/2$.

Varying pressure and temperature can violate conditions (3) and (4), resulting in a structural transition to a spontaneously deformed state that depends on the nonlinear elasticity of the material (the anharmonic expansion terms of the second, third, and higher orders) for its stability. Thus, the amount of spontaneous deformation that characterizes the new equilibrium structure is determined by the higher-order nonlinear contribution to the Gibbs energy. As shown by calculations, conditions (3a) and (4a), which correspond to the hydrostatic expansion compression, can only break down at negative pressures [15]. The spinodal instability at $P < 0$, when the lattice expansion is uniform, can be realized either in shock wave experiments [16] or by doping the crystal with atoms that exceed the host ones in size [17]. Therefore, the discussion that follows concerns conditions (3b) and (3c) and (4b)–(4d), which determine the stability of a crystal lattice toward shear.

Expansion (1) for the cubic and hexagonal lattices can be constructed using the results in Refs [18, 19], where all nonzero second-to-fourth order elastic constants for each of the 32 point symmetry groups were presented.

Table 1 lists different versions of spontaneous deformation that correspond to the situation where cubic and hexagonal crystals lose their stability when these conditions are violated. In the cases under consideration, thermodynamic potential expansion (1) takes the form

$$\frac{\Delta G(P, \eta, T)}{V_0} = \frac{1}{2}\,q\eta^2 + \frac{1}{3}\,v\eta^3 + \frac{1}{4}\,w\eta^4 + \ldots\,. \tag{5}$$

The values of the coefficients q, v, and w for each of the cases are given in Table 1, where $\tilde{C}_{\alpha\beta}$ are the isothermal effective elastic constants of the corresponding order at a pressure P in Voigt's notation. Also shown in the table are transformations that are possible in accordance with the group theoretical analysis of Bravais lattice symmetry properties for bcc, fcc, and hcp lattices losing stability to shear [20]. If the cubic term in expression (5) is zero (cases 2, 5, and 6 in Table 1), then a second-order phase transition can result from the violation of the corresponding stability condition.

We next see what happens if the cubic term in Eqn (5) is different from zero. Elastic constant calculations show that far from the point of stability loss, q and w are usually positive and v is negative. Equation (5) contains three parameters, each of which depends on P and T, thus complicating the analysis of the equation. However, after the two sides of this equation are divided by $G_0 = v^4/w^3$, it is reduced to a dimensionless single-coefficient form [21]

$$f(a, x) = a\,\frac{x^2}{2} - \frac{x^3}{3} + \frac{x^4}{4}\,, \tag{6}$$

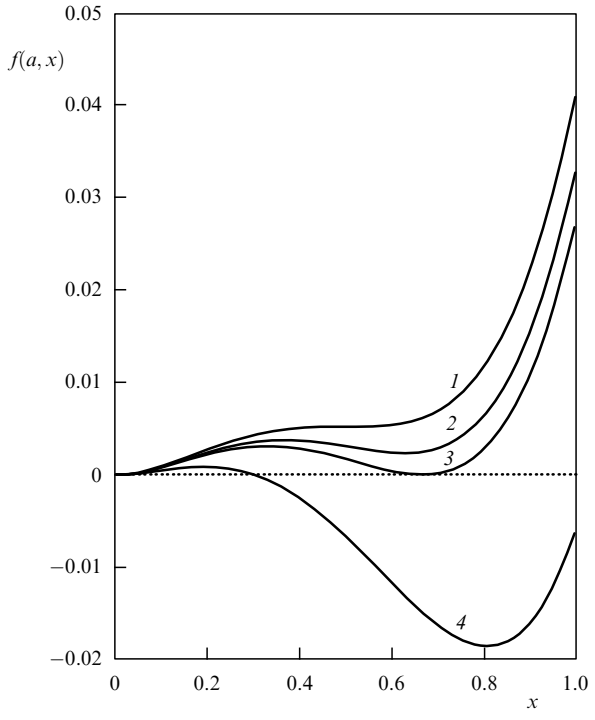

Figure 1. Dimensionless Gibbs potential for various values of the coefficient a: (*1*) $a = 1/4$; (*2*) $a = 2.1/9$; (*3*) $a = 2/9$; (*4*) $a = 1.4/9$.

where

$$f(a,x) = \frac{\Delta G}{V_0 G_0}\,, \qquad x = \frac{w}{|v|}\,\eta\,, \qquad a = \frac{qw}{v^2}\,. \tag{7}$$

The coefficient a accounts for the variation of the second-, third-, and fourth-order elastic constants with pressure and temperature, and its value determines the minimum–maximum pattern of Eqn (6) (Fig. 1). The positions of the minima and maxima are determined from the condition $\partial f/\partial x = 0$, leading to the equation $ax - x^2 + x^3 = 0$, which is solved by $x = 0$ and $x = (1 \pm \sqrt{1-4a}\,)/2$. It hence follows that for $a > 1/4$, the function $f(a,x)$ has only one minimum at $x = 0$, corresponding to the original phase. If $a = 1/4$, there is one minimum at $x = 0$ and an inflection point at $x = 1/2$ (Fig. 1, curve *1*). For $2/9 < a < 2/8\,(1/4)$, the curve $f(a,x)$ has two minima: one stable at $x = 0$ and one metastable at $x = (1 + \sqrt{1-4a}\,)/2$, and a local maximum at $x = (1 - \sqrt{1-4a}\,)/2$ (Fig. 1, curve *2*).

The value of a corresponding to a first-order phase transition is found by solving the system of equations $f(a,x) = 0$ and $\partial f/\partial x = 0$, to give $a = 2/9$. For this value, function (6) has two minima corresponding to $f(a,x) = 0$ at $x = 0$ and $x = 2/3$ and a maximum at $x = 1/3$ (see Fig. 1, curve *3*). The height of the potential barrier and the jump of the order parameter under this transition are estimated from Eqns (6) and (7), giving

$$\frac{\Delta G}{V_0} = \frac{1}{324}\,\frac{v^4}{w^3}\,, \qquad \eta = \frac{2|v|}{3w}\,. \tag{8}$$

We now find the entropy change

$$\Delta S = -\frac{1}{V_0}\left(\frac{\partial \Delta G}{\partial T}\right)_P$$

under the transition between two states related by the deformation $\eta = 2|v|/(3w)$. Substituting the value of η in Gibbs potential (5), taking the derivative with respect to the temperature, and expanding to the fourth order in the order parameters results in

$$\Delta S = -\frac{2}{9}\,\frac{\partial}{\partial T}\left(\frac{qv^2}{w^2}\right)_P + \frac{4}{81}\,\frac{\partial}{\partial T}\left(\frac{v^4}{w^3}\right)_P.$$

Table 1 lists expressions for q, v, and w for all the cases considered. Knowing the entropy change ΔS, it is easy to find the latent transition heat $\Delta Q = T\Delta S$. Thus, the height of the potential barrier, the jump of the order parameter, the change in entropy, and the latent transition heat are determined by relations between the third- and fourth-order elastic constant, i.e., by the nonlinear elasticity of the crystal lattice. From the expression for the parameter a in Eqn (7), we see that if the value of v is close to w (i.e., the third-order anharmonism and the fourth-order anharmonism contribute comparably), then a first-order phase transition can occur at sufficiently large values of q (the corresponding second-order elastic constant). The change in the unit-cell volume is a second-order effect in η because $\Delta V/V_0 = -2(\eta_{12}^2 + \eta_{13}^2 + \eta_{23}^2) + 8\eta_{12}\eta_{13}\eta_{23}$ (see Ref. [15]). Thus, the distortion of structure occurs in parallel with a small (second-order in deformation) but negative change in volume.

For $0 < a < 2/9$, in addition to the metastable minimum at $x = 0$, $f(a,x)$ also shows a stable minimum at $x > 2/3$ with a maximum $f(a,x) > 0$ for x between these minima (curve *4* in Fig. 1). We have a first-order phase transition close to a second-order transition because the potential barrier decreases as a decreases.

The range of values of a allowing a first-order phase transition is $0 < a \leqslant 2/9$ or, in terms of elastic constants, $0 < qw \leqslant (2/9)v^2$.

Thus, analyzing deformation phase transitions requires data on the second-to-fourth order elastic constants for different pressures. Unfortunately, high-pressure experimental data on crystal elastic constants of different orders are virtually absent, because the megabar range is a difficult one to measure the speed of sound in different crystallographic directions and to generate the second harmonic or Raman scattering normally used in determining elastic constants. Currently, the way to obtain sufficiently accurate second- and higher-order elastic constants at different pressures is by first-principle calculations within the electron density functional framework. This methodology is briefly discussed in Section 3 (see our paper [14] for the details).

3. Effective elastic constants

With the density functional method, it is possible to calculate the total energy of the crystal for any atomic volume (i.e., for any pressure). Accordingly, we express $\Delta G/V_0$ in terms of the change in the Helmholtz free energy ΔF. At a hydrostatic pressure P, we obtain

$$\frac{\Delta G}{V_0} = \frac{\Delta F}{V_0} + P\,\frac{\Delta V}{V_0}\,, \tag{9}$$

where $\Delta V = V - V_0$ is the change in the atomic volume due to the applied strain specified by the components of the

Table 2. $\tilde{C}_{\alpha\beta\ldots} - C_{\alpha\beta\ldots}$ relations.

$\tilde{C}_{\alpha\beta}$	$\tilde{C}_{\alpha\beta\gamma}$	$\tilde{C}_{\alpha\beta\gamma\delta}$	
$\tilde{C}_{11} = C_{11} - P$	$\tilde{C}_{111} = C_{111} + 3P$	$\tilde{C}_{1111} = C_{1111} - 15P$	$\tilde{C}_{4444} = C_{4444} - 3P$
$\tilde{C}_{12} = C_{12} + P$	$\tilde{C}_{112} = C_{112} - P$	$\tilde{C}_{1112} = C_{1112} + 3P$	$\tilde{C}_{4455} = C_{4455} - P$
$\tilde{C}_{44} = C_{44} - P$	$\tilde{C}_{123} = C_{123} + P$	$\tilde{C}_{1122} = C_{1122} + P$	$\tilde{C}_{6666} = C_{6666} - 3P$
	$\tilde{C}_{222} = C_{222} + 3P$		

tensor η_{ij}. The quantity $\Delta F/V_0$ can be written as [13]

$$\frac{\Delta F}{V_0} = -P\eta_{ii} + \frac{1}{2}\, C_{ijkl}\,\eta_{ij}\,\eta_{kl} + \frac{1}{6}\, C_{ijklmn}\,\eta_{ij}\,\eta_{kl}\,\eta_{mn} + \frac{1}{24}\, C_{ijklmnpq}\,\eta_{ij}\,\eta_{kl}\,\eta_{mn}\,\eta_{pq}\,, \tag{10}$$

where

$$C_{ijkl\ldots} = \frac{1}{V_0}\left(\frac{\partial^n F}{\partial\eta_{ij}\,\partial\eta_{kl}\ldots}\right)_0 . \tag{11}$$

The constants $C_{ijkl\ldots}$ are the extension of nth-order elastic constants introduced by Brugger [22] to the case of a loaded state and, while not determining the elastic properties of a crystal under loading completely [23], they can, unlike $\tilde{C}_{ijkl\ldots}$, satisfy the Cauchy relations.

We express the effective nth-order elastic constants $\tilde{C}_{ijkl\ldots}$ under hydrostatic load in terms of the corresponding Brugger elastic constants $C_{ijkl\ldots}$ and the pressure P. We note that $\Delta V/V_0 = J - 1$, where $J = \det|\alpha_{ij}|$ [13]. Here, $\alpha_{ki} = \partial r_k/\partial R_i$ is the deformation gradient, and r_k and R_i is the respective Cartesian coordinate of the selected point in the deformed and the original crystal. To obtain the required relations between $\tilde{C}_{ijkl\ldots}$ and $C_{ijkl\ldots}$, we express α_{ij} in terms of η_{ij}. The η_{ij} are related to α_{ij} by [13]

$$\eta_{ij} = \frac{1}{2}\left(\alpha_{ki}\alpha_{kj} - \delta_{ij}\right), \tag{12}$$

where δ_{ij} is the Kronecker symbol. In turn, α_{ij} can be expressed in terms of the displacement gradient $u_{ij} = \partial u_i/\partial R_j$ ($u_i = r_i - R_i$):

$$\alpha_{ij} = \delta_{ij} + u_{ij}\,. \tag{13}$$

As a result, $\eta_{ij} = (u_{ij} + u_{ji} + u_{ki}u_{kj})/2$. Because the deformations we consider in what follows are 'pure' (no rotations, $u_{ij} = u_{ji}$), we find that

$$\eta_{ij} = u_{ij} + \frac{1}{2}\, u_{ki}u_{kj}\,. \tag{14}$$

Inverting relation (12) using Eqns (13) and (14) and keeping terms through the fourth order in η_{ij} yields

$$\alpha_{ij} = \delta_{ij} + \eta_{ij} - \frac{1}{2}\,\eta_{ki}\,\eta_{kj} + \frac{1}{2}\,\eta_{rk}\,\eta_{ri}\,\eta_{kj} - \frac{5}{8}\,\eta_{kj}\,\eta_{mk}\,\eta_{mn}\,\eta_{ni}\,. \tag{15}$$

From Eqns (2), (9), (11), and (15), the relations between $\tilde{C}_{ijkl\ldots}$ and $C_{ijkl\ldots}$ are derived. The results obtained for the elastic constants from Table 1 are shown in Table 2 (in which the second-, third-, and fourth-order elastic constants are given in Voigt's notation).

To summarize, $\tilde{C}_{\alpha\beta\ldots}$ of any order can be calculated using expansion (10), in which the linear term determines the value of the pressure and the higher-order terms determine the corresponding elastic constants $C_{\alpha\beta\ldots}$ (Brugger elastic constants). This is followed by using the relations in Table 2 to find the effective elastic constants of the desired order.

4. High-pressure structural transformations in vanadium

Experimental studies of the structure of vanadium under pressure [24] have revealed a room temperature bcc–rhombohedral phase transition at $P = 69$ GPa. The experimenters ascribed the transition to the softening of the elastic constant $\tilde{C}_{44}$ and believed it to be of the second order due to the lack of a jump in volume. There is a vast first-principle literature [25–27] pointing to the $\tilde{C}_{44}$ softening behavior (i.e., to the elastic constant becoming negative) in the pressure range considered. We can use the calculations in Ref. [27] of the second-to-fourth order elastic constants for different pressures at $T = 0$ K to take a closer look at the structural transition from the bcc to the rhombohedral phase. Row 3 of Table 1 lists the necessary elastic constants. Knowing the values of these constants, it is possible to determine the coefficient a [see Eqns (6) and (7)] for various pressures in the neighborhood of the phase transition point (50–70 GPa). The results are: $P = 55$ GPa, $a = 3.9$; $P = 63$ GPa, $a = 1.4$; $P = 68$ GPa, $a = 0.21$. Thus, for $P \approx 68$ GPa, the coefficient a becomes equal to the critical value $a = 2/9$, and the bcc structure (Γ_c^v) can undergo a transition to the rhombohedral phase (Γ_{rh}) (see Table 1, row 3). From Eqn (8), we find the jump in the order parameter at this transition, $\eta_{12} = \eta_{13} = \eta_{23} = \eta/2 = (1/3)|v|/w = 0.0075$. The small value of the order parameter indicates that although the phase transition in vanadium is of the first order, it is close to a second-order transition. The results of this analysis agree with the available experimental data [24].

Density functional theory calculations in Refs [27, 28] of vanadium phonon dispersion at different pressures show that both branches of transverse modes (directions $\Gamma-H$ and $\Gamma-N$) related to the elastic constant $\tilde{C}_{44}$ exhibit strong softening near the center of the Brillouin zone (Γ point) at pressures from 70 GPa to 75 GPa. With further increasing the pressure, both branches continue decreasing in slope near this point. At the same time, the other transverse branch in the direction $\Gamma-N$ [the branch related to the elastic constant $\tilde{C}' = (\tilde{C}_{11} - \tilde{C}_{12})/2$] actually remains unchanged in this pressure range. Hence, the way the dispersion curves change with pressure agrees with the data on elastic constants.

5. Softening of the effective elastic constant $\tilde{C}'$ in molybdenum at high pressure

Figures 2–5 show our results [29] on the elastic constants and phonon dispersion relations in bcc molybdenum in the pressure range 0–1400 GPa ($T = 0$ K). We see from Fig. 2

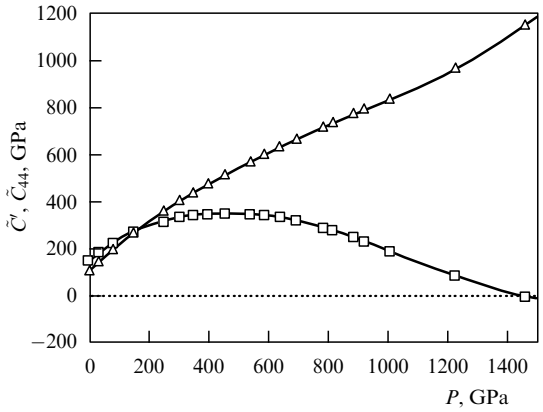

Figure 2. Pressure dependence of the shear elastic constants of bcc Mo; $\tilde{C}' = (\tilde{C}_{11} - \tilde{C}_{12})/2$ (squares) and $\tilde{C}_{44}$ (triangles).

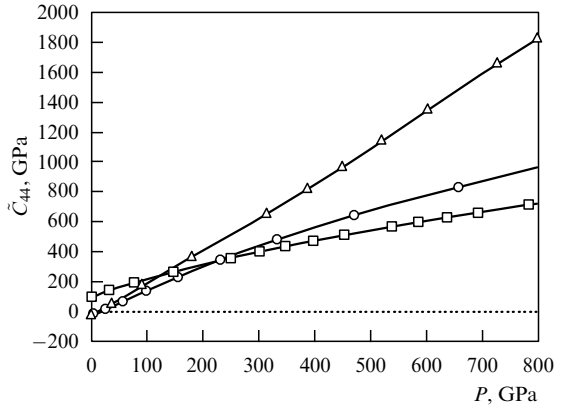

Figure 3. Elastic constant $\tilde{C}_{44}$ versus pressure for bcc (squares), fcc (circles), and hcp (triangles) molybdenum.

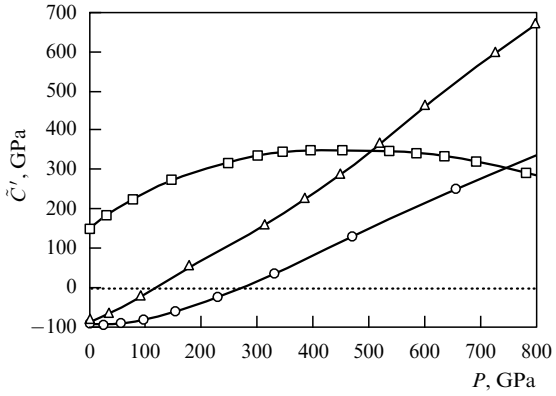

Figure 4. Elastic constant $\tilde{C}'$ versus pressure for bcc (squares), fcc (circles), and hcp (triangles) molybdenum.

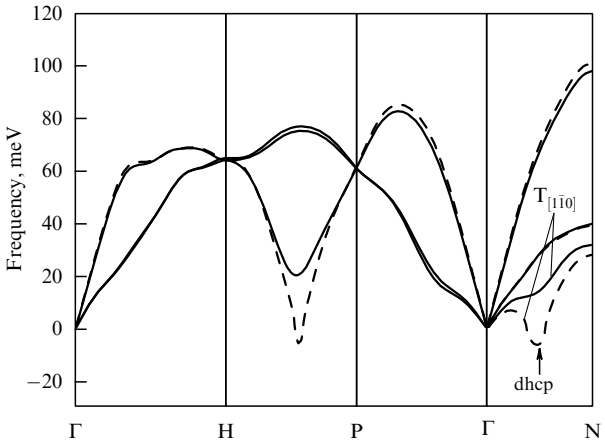

Figure 5. Phonon dispersion curves of bcc molybdenum under 900 GPa (solid curve) and 1050 GPa (dashed curve). Negative values correspond to imaginary values.

that for $P > 500$ GPa, $\tilde{C}'$ shows strong softening (a precursor of a phase transition) and passes through zero at $P \approx 1400$ GPa ($V/V_0 \approx 0.42$). At these pressures, molybdenum can undergo a deformation phase transition to a tetragonal or orthorhombic crystal structure [stability condition (3b) is violated)]. However, according to Refs [30–33], already at a pressure $P \approx 700$ GPa ($T = 0$ K), bcc molybdenum becomes thermodynamically unstable and must change to fcc or hcp. Estimates show that at these pressures, the coefficient a [see Eqn (6)] greatly exceeds 2/9, the critical value for the first-order deformation phase transition. Figures 3 and 4 show the calculated stability criteria (3b), (3c) and (4b), (4c) for bcc, fcc, and hcp molybdenum. It is seen that at atmospheric pressure, both fcc and hcp molybdenum structures are unstable to shear ($\tilde{C}_{44} < 0$ and $\tilde{C}' < 0$), and it is only at the respective high pressures $P \geqslant 300$ GPa and $P \geqslant 150$ GPA that they stabilize. From the standpoint of stability to uniform deformations in a phase transition, Figs 3 and 4 indicate the hexagonal structure to be preferable.

Figure 5 presents calculated phonon dispersion curves for bcc molybdenum in the pressure range 900–1050 GPa. We see that the transverse mode branch $T_{[1\bar{1}0]}[\zeta\,\zeta\,0]$ in the direction $\Gamma-\mathrm{N}$ related to the elastic constant $\tilde{C}'$ (the marked branch in Fig. 5) softens considerably near the Γ point at 900 GPA. Moreover, strong softening is also observed for the longitudinal branch $L[\zeta\,\zeta\,\zeta]$ in the direction $\mathrm{H}-\mathrm{P}$. As the pressure increases further and reaches $P = 1050$ GPa, the frequencies of these branches become imaginary near the vibrational modes

$$T_{[1\bar{1}0]}\left[\frac{1}{4}\,\frac{1}{4}\,0\right] \quad \text{and} \quad L\left[\frac{2}{3}\,\frac{2}{3}\,\frac{2}{3}\right].$$

It is shown in [17] that the instability of the bcc lattice to the vibrational mode $T_{[1\bar{1}0]}[1/4\ 1/4\ 0]$ (shown by an arrow in Fig. 5), combined with the softening of the shear elastic constant $\tilde{C}'$, can lead to a transition between bcc and double hcp (dhcp) structures.

Because of the small value of $\tilde{C}'$, the energy barrier for such a structural transformation is low. The transition itself is of the first order and occurs before the phonon mode in the original lattice becomes unstable. Thus, the structural transition in Mo to the double hcp phase should occur before the constant $\tilde{C}'$ becomes zero.

6. Conclusions

We have analyzed the stability of the crystal lattice to shear and examined elastic phase transitions at high pressures. Stability criteria against shear for cubic and hexagonal structures under pressure are expressed in terms of second-order effective elastic constants. Situations where these structures lose stability under hydrostatic pressure are

considered, and the Bravais lattices of higher-pressure phases resulting from elastic phase transitions are indicated. These phases depend on the nonlinear lattice elasticity for their stability. A criterion is given that indicates at what relation between the second-, third-, and fourth-order elastic constants a first-order elastic phase transition is possible. The jump in the order parameter and the height of the potential barrier at the transition are determined by the third- and fourth-order elastic constants. The elastic bcc-to-rhombohedral phase transition observed in vanadium at $P \approx 69$ GPa is analyzed, as are possible structural transformations in molybdenum at $P \geqslant 700$ GPa. We note that a similar analysis can be carried out for temperature-changing elastic phase transitions (martensitic transformations) if information is available on the second-to-fourth order elastic constants at around the transition temperature. Generally, elastic instability studies are important for explaining structural phase transitions in solids. A typical example is a pressure-induced transition in stishovite from the tetragonal structure to the orthorhombic $CaCl_2$-type structure [34].

Acknowledgments

Financial support from the Ministry of Education and Science of the Russian Federation under agreement 14.A18.21.0893 and from the Russian Foundation for Basic Research (grant Nos 13-02-00338 and 13-02-00844) is acknowledged.

References

1. Kolobyanina T N *Phys. Usp.* **45** 1203 (2002); *Usp. Fiz. Nauk* **172** 1361 (2002)
2. Maksimov E G, Magnitskaya M V, Fortov V E *Phys. Usp.* **48** 761 (2005); *Usp. Fiz. Nauk* **175** 793 (2005)
3. Katzke H, Tolédano P *Phys. Rev. B* **71** 184101 (2005)
4. Dubrovinsky L et al. *Nature Commun.* **3** 1163 (2012)
5. Bushman A V, Fortov V E *Sov. Phys. Usp.* **26** 465 (1983); *Usp. Fiz. Nauk* **140** 177 (1983)
6. Katsnelson M I et al. *Phys. Rev. B* **61** 14420 (2000)
7. Khmel'nitskii D E *Sov. Phys. Solid State* **16** 2079 (1975); *Fiz. Tverd. Tela* **16** 3188 (1974)
8. Liakos J K, Saunders G A *Philos. Mag. A* **50** 569 (1984)
9. Indenbom V L *Sov. Phys. Crystallogr.* **5** 106 (1960); *Kristallogr.* **5** (1) 115 (1960)
10. Cowley R A *Phys. Rev. B* **13** 4877 (1976)
11. Landau L D, Lifshitz E M *Statistical Physics* Vol. 1 (Oxford: Pegramon Press, 1980); Translated from Russian: *Statisticheskaya Fizika* Pt. 1 (Moscow: Nauka, 1976)
12. Sakhnenko V P, Talanov V M *Sov. Phys. Solid State* **21** 1401 (1979); *Fiz. Tverd. Tela* **21** 2435 (1979); *Fiz. Tverd. Tela* **22** 785 (1980)
13. Wallace D C, in *Solid State Phyicis* Vol. 25 (Eds H Ehrenreich, F Seitz, D Turnbull) (New York: Academic Press, 1970) p. 301
14. Krasil'nikov O M, Vekilov Yu Kh, Mosyagin I Yu *JETP* **115** 237 (2012); *Zh. Eksp. Teor. Fiz.* **142** 266 (2012)
15. Krasil'nikov O M et al. *JETP* **112** 240 (2011); *Zh. Eksp. Teor. Fiz.* **139** 281 (2011)
16. Sin'ko G V, Smirnov N A *JETP Lett.* **75** 184 (2002); *Pis'ma Zh. Eksp. Teor. Fiz.* **75** 217 (2002)
17. Grimvall G et al. *Rev. Mod. Phys.* **84** 945 (2012)
18. Huntington H B *Solid State Phys.* **7** 213 (1958); *Usp. Fiz. Nauk* **74** 303 (1961)
19. Chung D Y, Li Y *Acta Cryst. A* **30** 1 (1974)
20. Bir G L, Pikus G E *Symmetry and Strain-Induced Effects in Semiconductors* (New York: Wiley, 1974); Translated from Russian: *Simmetriya i Deformatsionnye Effekty v Poluprovodnikakh* (Moscow: Nauka, 1972)
21. Krumhansl J A, Gooding R J *Phys. Rev. B* **39** 3047 (1989)
22. Brugger K *Phys. Rev.* **133** A1611 (1964)
23. Martin J W *J. Phys. C Solid State Phys.* **8** 2837 (1975)
24. Ding Y et al. *Phys. Rev. Lett.* **98** 085502 (2007)
25. Landa A et al. *J. Phys. Condens. Matter* **18** 5079 (2006)
26. Koči L et al. *Phys. Rev. B* **77** 214101 (2008)
27. Krasilnikov O M et al. *J. Phys. Condens. Matter* **24** 195402 (2012)
28. Luo W et al. *Proc. Natl. Acad. Sci. USA* **104** 16428 (2007)
29. Krasilnikov O M et al. *Comput. Mater. Sci.* **81** 313 (2014)
30. Belonoshko A B et al. *Phys. Rev. Lett.* **92** 195701 (2004)
31. Belonoshko A B et al. *Phys. Rev. Lett.* **100** 135701 (2008)
32. Mikhaylushkin A S et al. *Phys. Rev. Lett.* **101** 049602 (2008)
33. Wang B, Zhang G B, Wang Y X *J. Alloys Compounds* **556** 116 (2013)
34. Shieh S R, Duffy T S, Li B *Phys. Rev. Lett.* **89** 255507 (2002)